3516 *Inorg. Chem.* **2010**, *49*, 3516–3524
DOI: 10.1021/ic1000649

Inorganic Chemistry
Article

Spin−Spin Interactions in Porphyrin-Based Monoverdazyl Radical Hybrid Spin Systems

Prashanth K. Poddutoori,[†] Melanie Pilkington,*[,†] Antonio Alberola,[‡,§] Victor Polo,[‡] John E. Warren,[⊥] and Art van der Est*[,†]

[†]*Department of Chemistry, Brock University, 500 Glenridge Avenue, St. Catharines, Ontario, L2S 3A1 Canada,* [‡]*Departamento de Quimica Fisica y Analitica, Universitat Jaume I, Avenida Sos Baynat s/n, Castellón, 12701 Spain, and* [⊥]*Daresbury Laboratory, CCLRC, Warrington, Cheshire, WA4 4AD. U.K..* [§] *Current address: Resenergie SL, C/Clariano 15, 46021 Valencia, Spain.*

Received January 11, 2010

The spin−spin interactions in a complex consisting of a metalloporphyrin with a verdazyl radical attached at one of the β positions of the porphyrin ring are investigated. The X-ray crystal structure of the copper porphyrin complex shows that the plane of the verdazyl moiety is oriented such that it is nearly perpendicular to the plane of the porphyrin ring so that weak magnetic interactions between the metal and radical are expected. Consistent with this expectation, magnetic susceptibility and continuous-wave electron paramagnetic resonance (EPR) measurements of the copper (d^9) and vanadyl (d^1) versions of the porphyrin show that the metal and radical are weakly antiferromagnetically coupled. Thus, the ground state is a singlet, but the triplet state is thermally accessible above ~5 K. Spin-polarized transient EPR measurements of the free-base analogue show that its lowest excited state is a quartet, indicating that the verdazyl radical couples ferromagnetically to the triplet excited state of the porphyrin. Low-temperature transient EPR measurements on the vanadyl porphyrin reveal that the lowest excited quintet state is populated. This implies that the antiferromagnetic coupling between the metal and radical observed in the ground state is switched to a ferromagnetic arrangement in the excited state by the presence of the unpaired electrons in the π and π^* orbitals of the porphyrin.

Introduction

The design of molecular systems with multiple spin centers that can be aligned via the exchange interaction has become an important field of study[1−12] because of the possible applications of such systems, for example, as storage devices. One well-established design approach[13−18] is to attach paramagnetic ligands to paramagnetic metal centers with the goal of creating a material in which the ligands mediate ferromagnetic coupling between the neighboring centers. The porphyrins are attractive building blocks for these kinds of complexes because of their extended π conjugation, their ability to bind a wide variety of metals, and the ease with which they can be functionalized.[19−31] Recent examples

*To whom correspondence should be addressed. E-mail: avde@brocku.ca.

(1) Goodwin, H. A. *Coord. Chem. Rev.* **1976**, *18*, 293–325.
(2) Gütlich, P.; Hauser, A.; Spiering, H. *Angew. Chem., Int. Ed. Engl.* **1994**, *33*, 2024–2054.
(3) Sato, O.; Iyoda, T.; Fujishima, A.; Hashimoto, K. *Science* **1996**, *272*, 704–705.
(4) Gütlich, P.; Garcia, Y.; Woike, T. *Coord. Chem. Rev.* **2001**, *219*, 839–879.
(5) Sato, O. *Acc. Chem. Res.* **2003**, *36*, 692–700.
(6) Sato, O. *J. Photochem. Photobiol. C* **2004**, *5*, 203–223.
(7) Gütlich, P.; Goodwin, H. A. Spin crossover—An overall perspective. *Spin Crossover in Transition Metal Compounds I*; Springer: New York, **2004**; Vol. *233*, pp 1−47.
(8) Mrozinski, J. *Coord. Chem. Rev.* **2005**, *249*, 2534–2548.
(9) Coronado, E.; Gatteschi, D. *J. Mater. Chem.* **2006**, *16*, 2513–2515.
(10) Einaga, Y. *J. Photochem. Photobiol. C* **2006**, *7*, 69–88.
(11) Blundell, S. J. *Contemp. Phys.* **2007**, *48*, 275–290.
(12) Halcrow, M. A. *Coord. Chem. Rev.* **2009**, *253*, 2493–2514.
(13) Pierpont, C. G.; Buchanan, R. M. *Coord. Chem. Rev.* **1981**, *38*, 45–87.
(14) Kaim, W. *Coord. Chem. Rev.* **1987**, *76*, 187–235.
(15) Caneschi, A.; Gatteschi, D.; Sessoli, R.; Rey, P. *Acc. Chem. Res.* **1989**, *22*, 392–398.
(16) Caneschi, A.; Gatteschi, D.; Rey, P. *Prog. Inorg. Chem.* **1991**, *39*, 331–429.
(17) Shultz, D. A. Valence Tautomerization in Dioxolene Complexes of Cobalt. In *Magnetism: Molecules to Materials II, Molecule-Based Materials*; Miller, J. S., Drillon, M., Eds.; Wiley-VCH: New York, 2001; pp 281−306.
(18) Koivisto, B. D.; Hicks, R. G. *Coord. Chem. Rev.* **2005**, *249*, 2612–2630.
(19) Miller, J. S.; Calabrese, J. C.; McLean, R. S.; Epstein, A. *J. Adv. Mater.* **1992**, *4*, 498–501.
(20) Miller, J. S.; Vazquez, C.; Jones, N. L.; McLean, R. S.; Epstein, A. J. *J. Mater. Chem.* **1995**, *5*, 707–711.
(21) O'Shea, D. F.; Miller, M. A.; Matsueda, H.; Lindsey, J. S. *Inorg. Chem.* **1996**, *35*, 7325–7338.
(22) Sugiura, K.; Arif, A. M.; Rittenberg, D. K.; Schweizer, J.; Ohrstrom, L.; Epstein, A. J.; Miller, J. S. *Chem.—Eur. J.* **1997**, *3*, 138–142.
(23) Wynn, C. M.; Girtu, M. A.; Brinckerhoff, W. B.; Sugiura, K. I.; Miller, J. S.; Epstein, A. J. *Chem. Mater.* **1997**, *9*, 2156–2163.
(24) Yates, M. L.; Arif, A. M.; Manson, J. L.; Kalm, B. A.; Burkhart, B. H.; Miller, J. S. *Inorg. Chem.* **1998**, *37*, 840–841.

Published on Web 03/10/2010

include porphyrins bearing phenyl carbene groups,[32,33] manganese(II) porphyrin−tetracyanoethylene complexes,[34] tetragalvinolphenyl and bis(semiquinone)porphyrin systems.[35,36] In π-conjugated molecular systems such as these, the relationship between the sign of the exchange coupling and the orbital topology is well understood.[37−39] However, controlling its magnitude is challenging because it is highly dependent on the molecular structure.[37,40,41] Studies of nitroxide-labeled metalloporphyrins and other transition-metal complexes with nitroxide-containing ligands show that the metal nitroxide spin−spin interactions depend critically on the nature of the ligand.[42,43] The magnitude of the exchange coupling between a metalloporphyrin π-cation radical and appended radicals has also been found to depend on the nature of the attached radical.[35,36] For many radicals, the bulky substituents that are required for chemical and thermal stability can also play a role in determining the nature and strength of the metal−ligand spin−spin interactions.

A further area of widespread interest is the development of molecular materials in which magnetic order can be induced using light.[2−6,10,12] This interest has led to a number of studies of the photophysics of systems consisting of a chromophore with attached stable radicals.[10,44−53] In these systems, the radical spins are usually weakly antiferromagnetically aligned in the ground state. However, when the chromophore is excited into its triplet state, the radicals couple more strongly and ferromagnetically to the triplet spin and, hence, ferromagnetic spin alignment of the radicals is induced. Transient electron paramagnetic resonance (TREPR) spectroscopy is an essential part of most of these studies because it is one of the few methods that can easily distinguish states of different spin multiplicities and allows the dynamics of the system to be followed. The spin-polarized TREPR spectra of the excited states of a number of chromophores with attached stable radicals have been reported[45−47,49,50,52,54−57] and used to study photoinduced spin alignment.[45,46,54,58] However, there are no TREPR studies of light-induced spin alignment in metal-radical-type systems in the literature. One reason for this is that transition metals typically have short spin-relaxation times and large hyperfine and/or zero-field splittings, which makes detection and analysis of spin-polarized spectra of metal complexes difficult. Recently, we demonstrated that, for vanadyl octaethylporphyrin, the spin relaxation is sufficiently slow that its spin-polarized excited quartet state can be detected by TREPR and that the time evolution and temperature dependence of the polarization gives a detailed picture of its excited-state dynamics.[59−61] A number of studies of light-induced spin polarization in copper porphyrin systems have also been reported over the past few years.[62−68] These results suggest that it may be possible to use TREPR spectroscopy to study light-induced spin alignment in metal-radical systems based on vanadyl and copper porphyrin.

(25) Brandon, E. J.; Rittenberg, D. K.; Arif, A. M.; Miller, J. S. *Inorg. Chem.* **1998**, *37*, 3376–3384.
(26) Johnson, M. T.; Arif, A. M.; Miller, J. S. *Eur. J. Inorg. Chem.* **2000**, 1781–1787.
(27) Rittenberg, D. K.; Sugiura, K.; Arif, A. M.; Sakata, Y.; Incarvito, C. D.; Rheingold, A. L.; Miller, J. S. *Chem.—Eur. J.* **2000**, *6*, 1811–1819.
(28) Mascarenhas, F.; Falk, K.; Klavins, P.; Schilling, J. S.; Tomkowicz, Z.; Haase, W. *J. Magn. Magn. Mater.* **2001**, *231*, 172–178.
(29) Ostrovsky, S.; Haase, W.; Drillon, M.; Panissod, P. *Phys. Rev. B: Condens. Matter Mater. Phys.* **2001**, 6413.
(30) Dawe, L. N.; Miglioi, J.; Turnbow, L.; Tallaferro, M. L.; Shum, W. W.; Bagnato, J. D.; Zakharov, L. N.; Rheingold, A. L.; Arif, A. M.; Fourmigue, M.; Miller, J. S. *Inorg. Chem.* **2005**, *44*, 7530–7539.
(31) Ikeue, T.; Furukawa, K.; Hata, H.; Aratani, N.; Shinokubo, H.; Kato, T.; Osuka, A. *Angew. Chem., Int. Ed.* **2005**, *44*, 6899–6901.
(32) Koga, N.; Iwamura, H. *Nippon Kagaku Kaishi* **1989**, 1456–1462.
(33) Iwamura, H. *Adv. Phys. Org. Chem.* **1990**, *26*, 179–253.
(34) Ribas-Arino, J.; Novoa, J. J.; Miller, J. S. *J. Mater. Chem.* **2006**, *16*, 2600–2611.
(35) Shultz, D. A.; Knox, D. A.; Morgan, L. W.; Sandberg, K.; Tew, G. N. *Tetrahedron Lett.* **1993**, *34*, 3975–3978.
(36) Shultz, D. A.; Mussari, C. P.; Ramanathan, K. K.; Kampf, J. W. *Inorg. Chem.* **2006**, *45*, 5752–5759.
(37) Rajca, A. *Chem. Rev.* **1994**, *94*, 871–893.
(38) Shultz, D. A. Conformational Exchange Modulation in Trimethylenemethane-Type Biradicals. In *Magnetic Properties of Organic Materials*; Lahti, P. M., Ed.; Dekker: New York, 1999; pp 103−126.
(39) Sugawara, T.; Matsushita, M. M. Localized spins exchange-coupled with itinerant electrons in organic π-electronic system. In *Carbon-Based Magnetism: an overview of the magnetism of metal free carbon-based compounds and materials*; Makarova, T., Palacio, F., Eds.; Elsevier: Amsterdam, The Netherlands, 2006; pp 1−22.
(40) Iwamura, H. *Proc. Jpn. Acad., Ser. B* **2005**, *81*, 233–243.
(41) Roques, N.; Gerbier, P.; Schatzschneider, U.; Sutter, J. P.; Guionneau, P.; Vidal-Gancedo, J.; Veciana, J.; Rentschler, E.; Guerin, C. *Chem.—Eur. J.* **2006**, *12*, 5547–5562.
(42) Eaton, S. S.; Eaton, G. R. *Coord. Chem. Rev.* **1978**, *26*, 207–262.
(43) Eaton, S. S.; Eaton, G. R. *Coord. Chem. Rev.* **1988**, *83*, 29–72.
(44) Mizuochi, N.; Ohba, Y.; Yamauchi, S. *J. Phys. Chem. A* **1999**, *103*, 7749–7752.
(45) Teki, Y.; Miyamoto, S.; Iimura, K.; Nakatsuji, M.; Miura, Y. *J. Am. Chem. Soc.* **2000**, *122*, 984–985.
(46) Conti, F.; Corvaja, C.; Toffoletti, A.; Mizuochi, N.; Ohba, Y.; Yamauchi, S.; Maggini, M. *J. Phys. Chem. A* **2000**, *104*, 4962–4967.
(47) Teki, Y.; Nakatsuji, M.; Miura, Y. *Mol. Phys.* **2002**, *100*, 1385–1394.
(48) Maretti, L.; Islam, S. S. M.; Ohba, Y.; Kajiwara, T.; Yamauchi, S. *Inorg. Chem.* **2005**, *44*, 9125–9127.
(49) Corvaja, C.; Conti, F.; Franco, L.; Maggini, M. *C. R. Chim.* **2006**, *9*, 909–915.
(50) Teki, Y.; Tamekuni, H.; Takeuchi, J.; Miura, Y. *Angew. Chem., Int. Ed.* **2006**, *45*, 4666–4670.
(51) Tarasov, V. F.; Saiful, I. S. M.; Ohba, Y.; Takahashi, K.; Yamauchi, S. *Spectrochim. Acta, Part A* **2008**, *69*, 1327–1330.
(52) Teki, Y.; Tamekuni, H.; Haruta, K.; Takeuchi, J.; Miura, Y. *J. Mater. Chem.* **2008**, *18*, 381–391.
(53) Ciofini, I.; Adamo, C.; Teki, Y.; Tuyeras, F.; Laine, P. P. *Chem.—Eur. J.* **2008**, *14*, 11385–11405.
(54) Teki, Y.; Nakatsuji, M.; Miura, Y. *Int. J. Mod. Phys. B* **2001**, *15*, 4029–4031.
(55) Franco, L.; Mazzoni, M.; Corvaja, C.; Gubskaya, V. P.; Berezhnaya, L. S.; Nuretdinov, I. A. *Appl. Magn. Reson.* **2006**, *30*, 577–590.
(56) Franco, L.; Mazzoni, M.; Corvaja, C.; Gubskaya, V. P.; Berezhnaya, L. S.; Nuretdinov, I. A. *Mol. Phys.* **2006**, *104*, 1543–1550.
(57) Binstead, R. A.; Crossley, M. J.; Hush, N. S. *Inorg. Chem.* **1991**, *30*, 1259–1264.
(58) Teki, Y.; Miyamoto, S.; Nakatsuji, M.; Miura, Y. *J. Am. Chem. Soc.* **2001**, *123*, 294–305.
(59) Kandrashkin, Y.; Asano, M. S.; van der Est, A. *Phys. Chem. Chem. Phys.* **2006**, *8*, 2129–2132.
(60) Kandrashkin, Y. E.; Asano, M. S.; van der Est, A. *J. Phys. Chem. A* **2006**, *110*, 9607–9616.
(61) Kandrashkin, Y. E.; Asano, M. S.; van der Est, A. *J. Phys. Chem. A* **2006**, *110*, 9617–9626.
(62) Asano-Someda, M.; van der Est, A.; Kruger, U.; Stehlik, D.; Kaizu, Y.; Levanon, H. *J. Phys. Chem. A* **1999**, *103*, 6704–6714.
(63) Asano-Someda, M.; Kaizu, Y. *Inorg. Chem.* **1999**, *38*, 2303–2311.
(64) Toyama, N.; Asano-Someda, M.; Ichino, T.; Kaizu, Y. *J. Phys. Chem. A* **2000**, *104*, 4857–4865.
(65) Asano-Someda, M.; Jinmon, A.; Toyama, N.; Kaizu, Y. *Inorg. Chim. Acta* **2001**, *324*, 347–351.
(66) van der Est, A.; Asano-Someda, M.; Ragogna, P.; Kaizu, Y. *J. Phys. Chem. A* **2002**, *106*, 8531–8542.
(67) Rozenshtein, V.; Berg, A.; Levanon, H.; Krueger, U.; Stehlik, D.; Kandrashkin, Y.; van der Est, A. *Isr. J. Chem.* **2003**, *43*, 373–381.
(68) Asano-Someda, M.; Toyama, N.; Kaizu, Y. *Appl. Magn. Reson.* **2003**, *23*, 393–407.

Scheme 1. Synthetic Scheme for the Verdazyl-Substituted Metalloporphyrins

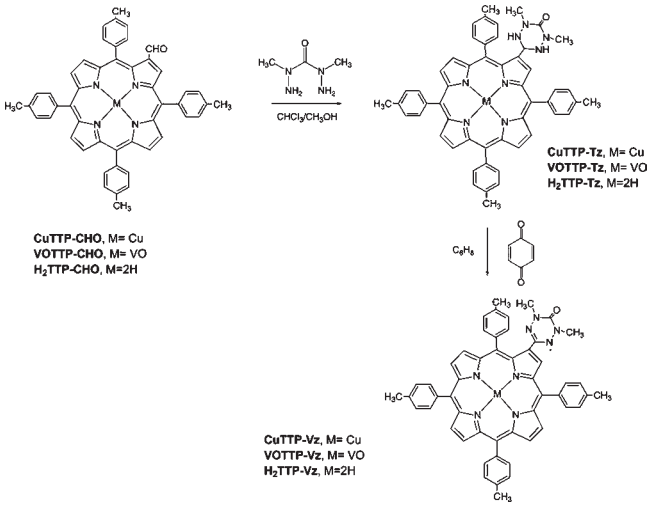

There has also been considerable interest recently in verdazyl radicals[18,69−84] as components of complexes with multiple spins because they are very stable and yet do not require bulky substituents for their stability. Thus, we have chosen to prepare and study a tetratolylporphyrin complex appended with a π-verdazyl radical (Vz) at one of the β-pyrrole ring positions as shown in Scheme 1. In the copper and vanadyl versions of the complex, magnetic susceptibility and continuous-wave electron paramagnetic resonance (CW EPR) data suggest that in the ground state the magnetic coupling between the verdazyl and metal spins is weak (< 10 cm^{-1}) and antiferromagnetic. On the other hand, spin-polarized TREPR data of the free-base version of the complex show that the radical couples ferromagnetically to the excited triplet state of the porphyrin ring. Similarly, it is known that the lowest excited state of the copper and vanadyl porphyrins is the so-called "tripquartet" state in which the metal is also ferromagnetically coupled to the excited triplet state of the porphyrin.[59,85] We will show that the spin-polarized TREPR spectrum of the excited quintet state is observable in the vanadyl version of the Vz-appended porphyrin. This implies that excitation of the π system aligns the metal and radical spins and changes the coupling between them from antiferromagnetic to ferromagnetic.

Experimental Section

X-ray Structural Analysis. Data were collected at 150 K using synchrotron radiation at Daresbury SRS, Cheshire, U.K. (Station 9.8), with a Bruker-Nonius APEX II CCD diffractometer ($\lambda = 0.6934$ Å), and the structure was solved by direct methods. All calculations were carried out using the *SHELXTL* package. Crystal data for CuTTP-Vz [$C_{52}H_{41}N_8OCu$]: $M =$ 857.47, monoclinic, $a = 33.003(6)$ Å, $b = 8.7240(11)$ Å, $c = 15.294(2)$ Å, $\beta = 91.376(6)°$, $V = 4402.3(12)$ Å^3, space group $P2_1/c$, $Z = 4$, 6249 reflections measured, R1 = 0.1029 [$I > 2\sigma(I)$].

Magnetic Susceptibility Measurements. Magnetic susceptibility measurements were made on a Quantum Design SQUID magnetometer in an applied field of 100 G between 3 and 300 K on 8 mg (CuTTP-Vz) and 9 mg (VOTTP-Vz) of polycrystalline sample. Data were corrected for both sample diamagnetism (Pascal's constants) and the sample holder.

EPR Measurements. EPR samples were prepared by dissolving the porphyrin complex under study in dichloromethane, toluene, or the liquid-crystalline solvent *p*-(*n*-pentyl)cyanobiphenyl (5CB). The solutions were placed in Suprasil EPR sample tubes (4 mm o.d.) and were degassed by several freeze−pump−thaw cycles and then sealed under vacuum. Transient EPR time/field data sets were recorded at either 80 or 20 K using a modified Bruker EPR 200D-SRC X-band spectrometer. Optical excitation at 532 nm was achieved using 10 ns pulses from a Nd:YAG laser at a repetition rate of 10 Hz. Steady-state Q-band (35 GHz) EPR spectra were collected using the same spectrometer operating in CW mode with a Bruker ER 051QR bridge and a ER 5106 QT-W resonator. X-band steady-state EPR spectra were collected at 120 K on a Bruker Elexsys E580 spectrometer.

Results and Discussion

Preparation of MTTP-Vz. The synthetic pathway to CuTTP-Vz, VOTTP-Vz, and H_2TTP-Vz is shown in Scheme 1 and is described in detail in the Supporting Information. Briefly, the desired β-substituted porphyrin-based monoverdazyl radicals were obtained from the corresponding 2-formylporphyrins[86] by reaction with bis(1-methylhydrazide)carbonic acid to give the 2-tetrazone porphyrin (MTTP-Tz), which was then oxidized to the verdazyl radical using benzoquinone. All compounds were purified by flash chromatography prior to the spectroscopic studies. The free-base porphyrin (H_2TTP-Vz) was found to be unstable as a solid after column purification, although it was stable for several days as a pure solution and as a solid prior to purification. Thus, it appears that the compound decomposes when the solid is formed from a pure solution but is stable when it is formed from the reaction mixture. We speculate that this is because hydroquinone, which is present in the reaction mixture, stabilizes the solid, as has been observed for

(69) Brook, D. J. R.; Lynch, V.; Conklin, B.; Fox, M. A. *J. Am. Chem. Soc.* **1997**, *119*, 5155–5162.
(70) Brook, D. J. R.; Fornell, S.; Noll, B.; Yee, G. T.; Koch, T. H. *J. Chem. Soc., Dalton Trans.* **2000**, 2019–2022.
(71) Brook, D. J. R.; Fornell, S.; Stevens, J. E.; Noll, B.; Koch, T. H.; Eisfeld, W. *Inorg. Chem.* **2000**, *39*, 562–567.
(72) Barclay, T. M.; Hicks, R. G.; Lemaire, M. T.; Thompson, L. K. *Chem. Commun.* **2000**, 2141–2142.
(73) Hicks, R. G.; Lemaire, M. T.; Thompson, L. K.; Barclay, T. M. *J. Am. Chem. Soc.* **2000**, *122*, 8077–8078.
(74) Barclay, T. M.; Hicks, R. G.; Lemaire, M. T.; Thompson, L. K. *Inorg. Chem.* **2001**, *40*, 6521–6524.
(75) Barclay, T. M.; Hicks, R. G.; Lemaire, M. T.; Thompson, L. K. *Inorg. Chem.* **2001**, *40*, 5581–5584.
(76) Barclay, T. M.; Hicks, R. G.; Lemaire, M. T.; Thompson, L. K.; Xu, Z. Q. *Chem. Commun.* **2002**, 1688–1689.
(77) Brook, D. J. R.; Abeyta, V. *J. Chem. Soc., Dalton Trans.* **2002**, 4219–4223.
(78) Barclay, T. M.; Hicks, R. G.; Lemaire, M. T.; Thompson, L. K. *Inorg. Chem.* **2003**, *42*, 2261–2267.
(79) Wu, J. Z.; Bouwman, E.; Reedijk, J.; Mills, A. M.; Spek, A. L. *Inorg. Chim. Acta* **2003**, *351*, 326–330.
(80) Hicks, R. G.; Koivisto, B. D.; Lemaire, M. T. *Org. Lett.* **2004**, *6*, 1887–1890.
(81) Lemaire, M. T.; Barclay, T. M.; Thompson, L. K.; Hicks, R. G. *Inorg. Chim. Acta* **2006**, *359*, 2616–2621.
(82) Koivisto, B. D.; Ichimura, A. S.; McDonald, R.; Lemaire, M. T.; Thompson, L. K.; Hicks, R. G. *J. Am. Chem. Soc.* **2006**, *128*, 690–691.
(83) Gilroy, J. B.; Koivisto, B. D.; McDonald, R.; Ferguson, M. J.; Hicks, R. G. *J. Mater. Chem.* **2006**, *16*, 2618–2624.
(84) Train, C.; Norel, L.; Baumgarten, M. *Coord. Chem. Rev.* **2009**, *253*, 2342–2351.
(85) Gouterman, M.; Mathies, R. A.; Smith, B. E.; Caughey, W. S. *J. Chem. Phys.* **1970**, *52*, 3795–3802.
(86) Barr, C. L.; Chase, P. A.; Hicks, R. G.; Lemaire, M. T.; Stevens, C. L. *J. Org. Chem.* **1999**, *64*, 8893–8897.

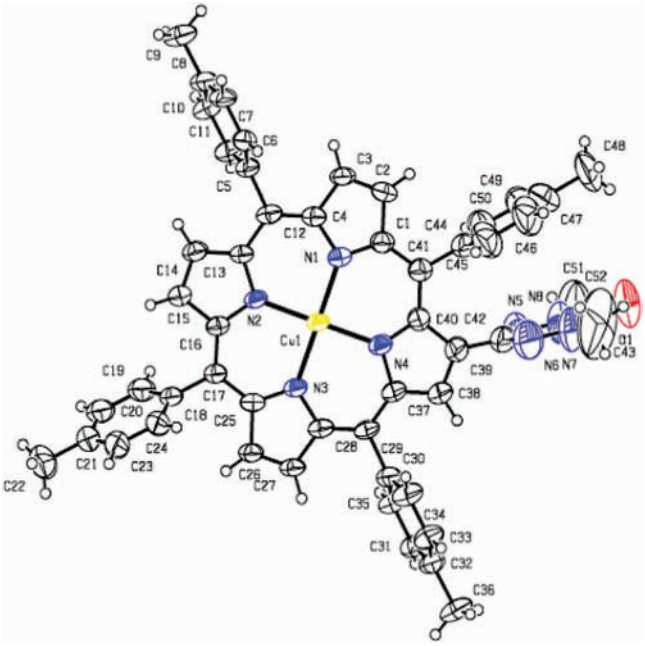

Figure 1. X-ray crystal structure of CuTTP-Vz. Atomic displacement parameters are plotted at 50%. Drawn with PLATON.

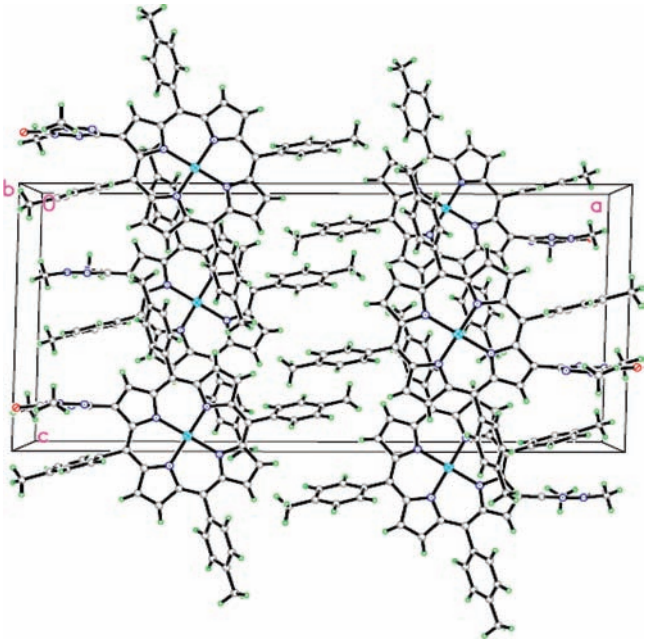

Figure 2. Packing diagram for CuTTP-Vz. A portion of the X-ray structure viewed along the *c* axis is shown.

other verdazyl compounds.[87] In contrast, VOTTP-Vz and CuTTP-Vz were found to be stable after column purification both in solution and as solids. Air-stable single crystals of CuTTP-Vz were isolated via the slow evaporation of a solution of the compound in a 1:1 mixture of dichloromethane and hexane at room temperature. However, no single crystals suitable for X-ray analysis could be obtained for VOTTP-Vz and H_2TTP-Vz.

X-ray Crystal Structure of CuTTP-Vz. The X-ray crystal structure of CuTTP-Vz shown in Figure 1 reveals that in the solid state the porphyrin ring is planar. The copper ion deviates from the plane of the porphyrin ring by only 0.006 Å. The Cu−N bond lengths are 1.985, 2.001, 2.001, and 2.006 Å. The phenyl rings are tilted by an angle of 74° with respect to the plane of the porphyrin ring. The shortest intermolecular distance between neighboring phenyl rings is 6.290 Å. The verdazyl ring is approximately perpendicular to the porphyrin ring but shows a significant deviation from this geometry, with the mean planes of the two rings being oriented at an angle of 84° with respect to one another. The internal structural parameters for the verdazyl moiety are within the normal range for such species;[78] the carbonyl and two methyl groups deviate by 0.175 (O1), 4.178 (C48), and 0.067 (C51) Å from the verdazyl plane, and the methyl groups are disordered. The verdazyl radical is eclipsed with the neighboring tolyl group at the meso position of the porphyrin ring (Figure 1) such that the planes of the two rings are at an angle of 16° with respect to one another and the average between them is 3.388 Å. The highest spin density for the unpaired electron on the verdazyl moiety is expected on the four nitrogen atoms, and their average distance from the spin bearing copper is 6.970 Å.

The crystal packing in the solid is shown in Figure 2. The copper porphyrin has an extended zigzag, one-dimensional network structure that runs along the *a* axis of the unit cell. As is evident from Figure 2, each CuTTP-Vz molecule has no direct overlap with its neighbor, but there are edge−edge interactions for which the C···C inter-ring distances range from 3.27 to 4.87 Å. The shortest Cu−Cu distances are 8.724 and 8.803 Å. There are no direct intermolecular interactions between neighboring verdazyl radicals in the solid state because of the intervening phenyl groups. The shortest intermolecular verdazyl radical to verdazyl radical distance is 7.8 Å.

CW EPR Spectra of CuTTP-Vz and VOTTP-Vz. Figure 3 shows CW EPR spectra of CuTTP-CHO, CuTTP-Vz, VOTTP-CHO, and VOTTP-Vz in a frozen toluene solution along with corresponding calculated spectra. As is evident, in Figure 3, introduction of the verdazyl group has a large impact on the *g* factors and hyperfine splittings as a result of the coupling between the radical and metal. With the nearly perpendicular orientation of the verdazyl and porphyrin rings seen in the X-ray crystal structure of CuTTP-Vz, there should be very little overlap of the orbital carrying the unpaired electron on the verdazyl radical with that of the odd d electron on the metal. Thus, the exchange interaction between the spins should be relatively weak. On the other hand, the Cu−verdazyl distance is sufficiently short that the spin−spin interaction should be large enough to separate the spin states in CuTTP-Vz and VOTTP-Vz into singlet and triplet manifolds, as seen for a wide range of nitroxide-labeled copper and vanadyl porphyrins.[42,43] Under these conditions, their CW EPR spectra arise from the triplet state. The spin Hamiltonians of the doublet state of MTTP-CHO and the triplet state of MTTP-Vz can be written as

$$H_D = \hbar(\omega_M S_{Mz} + \vec{S}_M \mathbf{A}_M \vec{I}) H_T$$
$$= \hbar(\omega_T S_{Tz} + \vec{S}_T \mathbf{A}_T \vec{I} + \vec{S}_T \mathbf{D} \vec{S}_T) \quad (1)$$

(87) Hicks, R. G.; Lemaire, M. T.; Ohrstrom, L.; Richardson, J. F.; Thompson, L. K.; Xu, Z. Q. *J. Am. Chem. Soc.* **2001**, *123*, 7154–7159.

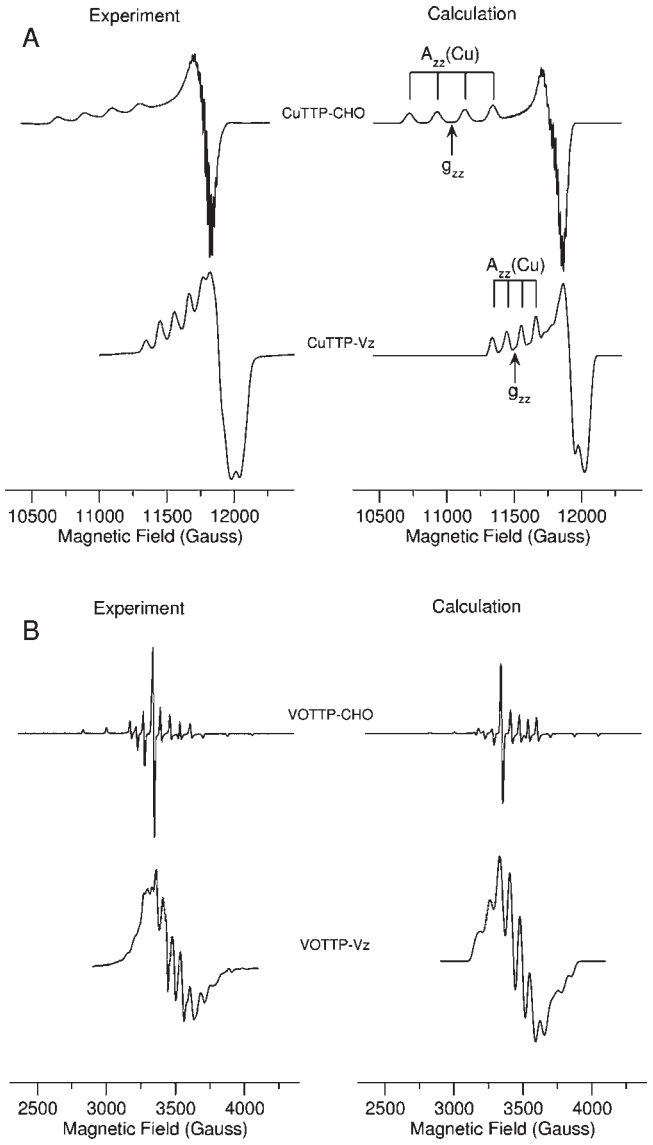

Figure 3. CW EPR spectra of MTTP-CHO and MTTP-Vz. A: Q-band CW EPR spectra of CuTTP-CHO and CuTTP-Vz. Left: experimental spectra taken at 80 K in toluene. Right: simulated spectra with g_{xx}(Cu) = g_{yy}(Cu) = 2.055, g_{zz}(Cu) = 2.186, A_{xx}(Cu) = A_{yy}(Cu) = 3.43 mT, A_{zz}(Cu) = 20.62 mT, g(Vz) = 2.0037, D(Cu,Vz) = −8.59 mT, J(Cu,Vz) > 1200 mT, and the angle between z and the dipolar coupling axis θ_{zD} = 80°. B: X-band CW EPR spectra of VOTTP-CHO and VOTTP-Vz. Left: experimental spectra taken at 80 K in toluene. Right: simulated spectra. g_{xx}(VO) = g_{yy}(VO) = 1.960, g_{zz}(Cu) = 1.927, A_{xx}(VO) = A_{yy}(VO) = 5.3 mT, A_{zz}(VO) = 17.8 mT, g(Vz) = 2.0037, D(Cu,Vz) = −8.59 mT, J(Cu,Vz) > 1200 mT, and the angle between z and the dipolar coupling axis θ_{zD} = 70°.

where the subscripts T and M refer to the triplet state and the metal spin, respectively, ω_T and ω_M are the corresponding resonance field positions, and **A** and **D** are the hyperfine coupling and zero-field-splitting (ZFS) tensors, respectively. For the triplet state, the values of the resonance field position ω_T and hyperfine interaction $\mathbf{A}_T$ can be related to the corresponding values for the metal and verdazyl radical:

$$\omega_T = \frac{1}{2}(\omega_M + \omega_{Vz}) \qquad \mathbf{A}_T = \frac{1}{2}\mathbf{A}_M \tag{2}$$

where

$$\omega_{M,Vz} = g_{M,Vz}\beta B \tag{3}$$

are the resonance frequencies for the metal spin (subscript M) and the unpaired electron of the verdazyl radical (subscript Vz). For the copper porphyrin case, the z component of the copper **g** tensor (g_{zz}) is well-resolved in the Q-band spectrum (Figure 3A) and is split into four peaks by hyperfine coupling to the spin $^3/_2$ copper nucleus [A_{zz}(Cu)] as indicated. Introduction of the verdazyl radical reduces the hyperfine coupling by a factor of 2 and causes a shift of the z component of the **g** tensor (g_{zz}) as predicted by eq 2. The simulations in Figure 3 are in good agreement with the experimental spectra and show that for both CuTTP-Vz and VOTTP-Vz the triplet state is observed. Thus, we can conclude that the exchange coupling between the spins is large relative to the difference in their precession frequencies,[43] and hence J must be larger than ∼0.5 cm^{-1}. However, the spectra do not indicate whether the triplet or singlet is lower in energy, and only show that the triplet state is populated under the conditions used.

Magnetic Susceptibility of CuTTP-Vz. Solid-state magnetic susceptibility data for CuTTP-Vz are shown in Figure 4A and provide additional information about the strength and sign of the spin−spin coupling. The corresponding data for VOTTP-Vz (not shown) are very similar. The plot in Figure 4A indicates that above 5 K the material is essentially paramagnetic and the susceptibility follows typical Curie−Weiss behavior with a Curie constant of 0.750 emu·K/mol. This value is twice that expected for a single $S = {}^1/_2$ spin, confirming the presence of two unpaired electrons per molecule and indicating that the spin−spin couplings in the solid are less than kT in this temperature range, i.e., $|J| < \sim 7$ cm^{-1}. The small value for the Weiss constant (−0.3 K) indicates the presence of weak antiferromagnetic interactions. This behavior is consistent with the X-ray crystal structure (Figures 1 and 2) because the verdazyl radical is oriented perpendicular to the porphyrin ring, preventing orbital overlap with the metal, and the toluene groups on the porphyrin hinder close interactions between neighboring verdazyl radicals. Thus, the susceptibility data suggest that for CuTTP-Vz and VOTTP-Vz the singlet state probably lies slightly below the triplet state, which is observed by EPR because it is thermally populated.

Temperature Dependence of the EPR Signal Intensity. The temperature dependence of the CW EPR signal provides an additional avenue by which the strength and sign of the spin−spin coupling can be estimated. For a system comprised of a singlet and triplet state, the intensity of the EPR signal of the triplet state is given by

$$I \propto \frac{e^{J/kT}(1 - e^{-\omega_T/kT})}{\sum_{i=1,4} e^{-E_i/kT}} \tag{4}$$

where J is the singlet−triplet energy gap, positive J places the singlet at higher energy than the triplet, and E_i refers to the energies of the three triplet sublevels and the singlet

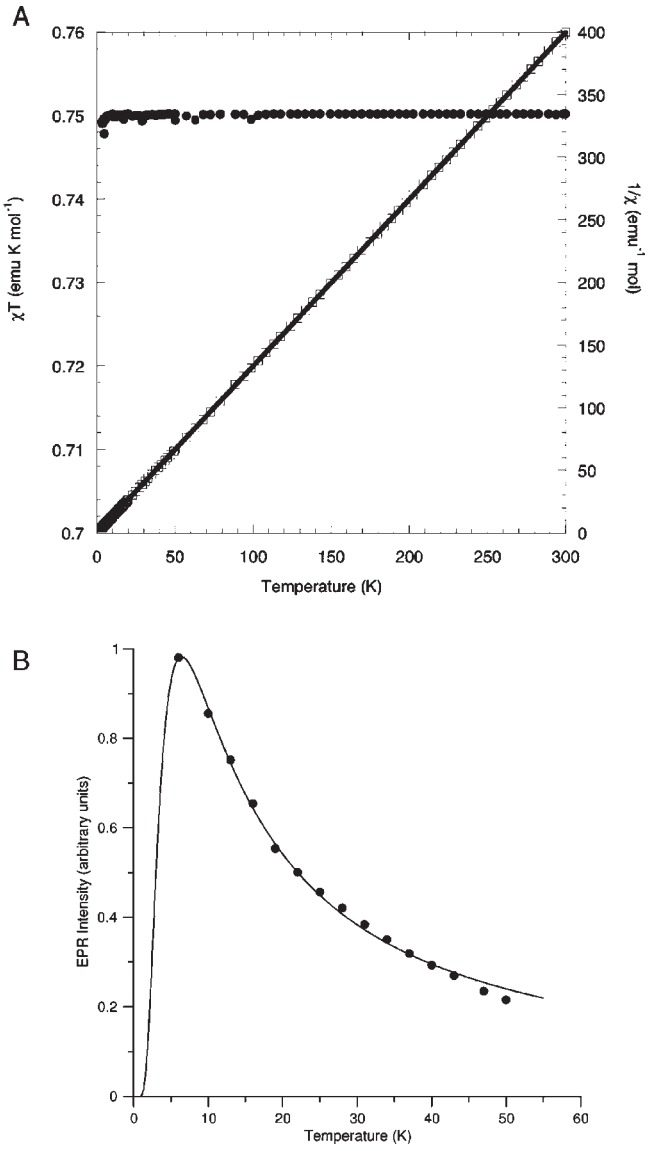

Figure 4. Magnetic susceptibility and CW EPR intensity of CuTTP-Vz. A: Temperature dependence of the magnetic susceptibility. Open squares: $1/\chi$ vs T with a fit to the Curie−Weiss law (gray solid line). Closed circles: χ vs T. B: Temperature dependence of the intensity of the EPR spectrum. The solid curve is a fit to the data with $J = -6.95$ cm^{-1}, where J is the singlet−triplet energy gap and negative J indicates that the singlet lies energetically below the triplet.

state. Here, we have assumed that the ZFS and hyperfine interactions can be ignored relative to the Zeeman energy and other electronic states carry no significant population. Figure 4B shows a plot of the temperature dependence of the intensity of the X-band spectrum of CuTTP-Vz and a fit of eq 1 to the experimental data. The fit yields a value of $J = -6.59$ cm^{-1} and indicates that the two spins couple antiferromagnetically in agreement with the susceptibility data. Positive values for J (ferromagnetic coupling) are not consistent with the data. Thus, together the EPR and susceptibility data indicate that the molecule has a singlet ground state and that the strength of the coupling between the metal and verdazyl radical is approximately 5−10 wavenumbers.

Transient EPR Spectrum of H_2TTP-Vz. Figure 5 shows the spin-polarized transient EPR spectra of H_2TTP-CHO

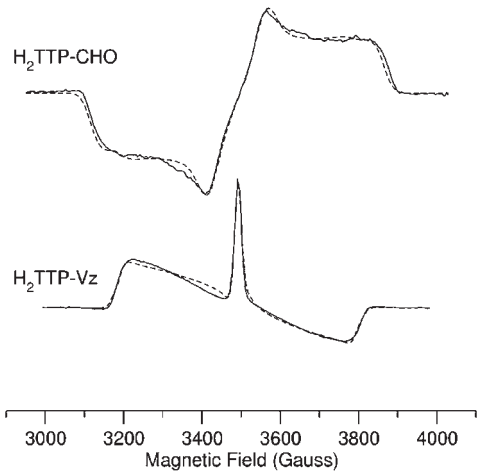

Figure 5. Spin-polarized transient EPR spectra of H_2TTP-CHO and H_2TTP-Vz. Solid curves: experimental spectra in a time window centerd at 860 ns after the laser flash measured at 80 K in toluene. Dashed curves: calculated spectra. Top: triplet state of H_2TTP-CHO, D = 34.8 mT, E = 7 mT, $\kappa_{m,P} = -1.0$, $\kappa_{m,\perp} = 0.20$, and $\kappa_n = 0.0$. Bottom: quartet state of H_2TTP-Vz, D = 16.0 mT, E = 4.6 mT, $\kappa_{m,P} = 1.0$, $\kappa_{m,\perp} = 0.68$, and $\kappa_n = -0.29$.

(top) and H_2TTP-Vz (bottom) measured in a toluene solution. The dashed lines are simulations calculated as described for vanadyl octaethylporphyrin.[60,88] In short, the spin polarization is calculated as the traceless diagonal part of the reduced density matrix for the observed state, $\Delta\rho$, which is written as a linear combination of contributions of different symmetries. Spin−orbit coupling intersystem crossing (ISC) produces multiplet polarization that is described by two terms that follow the internal symmetry of the molecule:

$$\begin{aligned}\Delta\rho_{m,\parallel} &= \frac{3}{2}(\cos^2\theta - 1/3)\left(S_z^2 - \frac{1}{3}\vec{S}^2\right)\\ \Delta\rho_{m,\perp} &= \frac{3}{2}(\sin^2\theta\cos 2\varphi)\left(S_z^2 - \frac{1}{3}\vec{S}^2\right)\end{aligned} \quad (5)$$

where θ and ϕ describe the orientation of the magnetic field relative to molecular axes. We also allow for net polarization, which is given by

$$\Delta\rho_n = S_z \quad (6)$$

The overall population distribution is a weighted sum of these three contributions:

$$\Delta\rho \propto \kappa_{m,\parallel}\Delta\rho_{m,\parallel} + \kappa_{m,\perp}\Delta\rho_{m,\perp} + \kappa_n\Delta\rho_n \quad (7)$$

and the weighting coefficients $\kappa_{m,\parallel}$, $\kappa_{m,\perp}$, and κ_n are treated as adjustable parameters.

The top spectrum in Figure 5 is that of the excited triplet state of H_2TTP-CHO, and the polarization pattern indicates that it is populated via ISC. Introduction of the verdazyl radical is expected to split the triplet state into so-called tripdoublet and tripquartet states, as observed for a number of other chromophores with an attached

(88) Kandrashkin, Y.; van der Est, A. *J. Chem. Phys.* **2004**, *120*, 4790–4799.

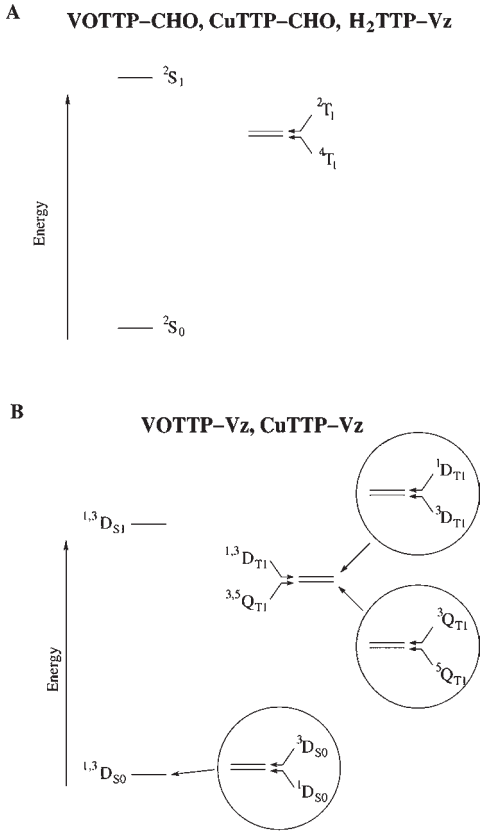

Figure 6. Jablonski diagrams. A: Diagram for porphyrins such as those of VOTTP-CHO, CuTTP-CHO, or H_2TTP-Vz with a paramagnetic metal or radical with spin $^1/_2$. The energy levels are drawn approximately to scale using the reported values for copper porphine.[99] For H_2TTP-Vz, the energy gap between the tripdoublet ($^2T_1$) and tripquartet ($^4T_1$) states is smaller than that shown. B: Diagram for porphyrins such as CuTTP-Vz and VOTTP-Vz, which contain both a paramagnetic metal and a free radical. The energy levels shown in the circles are drawn on an expanded energy scale to show the weak splitting due to the verdazyl radical.

radical.[44,46,47,49,52,89−93] This results in an energy-level scheme analogous to that of CuTTP-CHO and VOTTP-CHO, as shown in the Jablonski energy diagram in Figure 6A. If the tripquartet ($^4T_1$) lies below the tripdoublet ($^2T_1$), i.e., if the triplet−doublet exchange coupling is positive, the excited singdoublet state ($^2S_1$) is expected to relax rapidly to the tripdoublet, which then decays to the tripquartet by spin−orbit-coupling-mediated ISC.[64,94] Recently, we calculated the spin polarization expected in the tripquartet for this mechanism[88,95] and showed that this process also leads to net polarization of the quartet state. The net polarization is predicted to be absorptive, and it results in a sharp absorptive peak in the center of the spectrum due to the transitions between the $m_s = \pm^1/_2$ sublevels of the tripquartet. The spectrum of H_2TTP-Vz (Figure 5, bottom) is simulated assuming that it arises solely from the tripquartet state with multiplet and net polarization contributions as described above. As can be seen in Figure 5, the simulations (dashed curves) are in good agreement with the experimental spectra (solid curves). Hence, we conclude that the spectrum arises only from the tripquartet, which lies energetically below the tripdoublet. This means that the triplet spin and the verdazyl radical spin couple ferromagnetically, i.e., positive J. The polarization pattern and line shape suggest that the magnitude of J is larger than the Zeeman energy but do not allow its value to be determined. However, it is reasonable to assume that it is as large or larger than the coupling between the verdazyl radical and the copper metal in CuTTP-Vz. On the other hand, it is expected to be weaker than the triplet−doublet coupling in CuTTP or VOTTP, which places it in the range of 10−100 wavenumbers.[85] The ZFS of the tripquartet is given by

$$D_{Qa} = \frac{1}{3}(D_T + D_{TD}) \quad (8)$$

where D_T is the ZFS parameter of the triplet excitation and D_{TD} is the dipolar coupling between the triplet and doublet. From the simulations shown in Figure 5, we evaluate $D_{Qa} = 16.0$ mT and $D_T = 34.8$ mT, which yields $D_{TD} = 13.2$ mT.

Transient EPR Spectra of VOTTP-Vz. Excitation of VOTTP-Vz generates a system of four coupled unpaired electrons: two on the porphyrin in the π and π^* orbitals, one on the vanadyl center, and one on the verdazyl moiety. The coupling between the π and π^* electrons is ferromagnetic and is known to be on the order of ~4000 cm^{-1} in metalloporphyrins.[96] From optical studies of copper and vanadyl porphyrins, it is known that the coupling between the metal spin and the triplet excitation of the porphyrin is also ferromagnetic and on the order of 100−300 cm^{-1}.[85,97] As shown above, the unpaired electron of the verdazyl radical couples ferromagnetically to the triplet excitation of the porphyrin but antiferromagnetically to the metal. It is not possible to satisfy all of these couplings simultaneously, and the alignment of the most weakly coupled spins is expected to change in the lowest excited state of VOTTP-Vz. The resulting energy diagram is shown in the Jablonski diagram (Figure 6B). The EPR and magnetic susceptibility data suggest that the coupling between the metal and verdazyl radical is weak (5−10 cm^{-1}), and although we expect the coupling between the porphyrin triplet spin and the radical to be stronger, it is not certain which orientation the radical spin will take relative to the metal and triplet spins in the lowest excited state. As shown in Figure 6B, the coupling to the radical splits the tripquartet into a quintet ($^5Q_{T1}$) and a triplet state ($^3Q_{T1}$). We have indicated the quintet as the lowest excited state, but it is also possible that the order is reversed and the quintet lies above the triplet.

(89) Ishii, K.; Fujisawa, J.; Ohba, Y.; Yamauchi, S. *J. Am. Chem. Soc.* **1996**, *118*, 13079–13080.
(90) Fujisawa, J.; Ishii, K.; Ohba, Y.; Yamauchi, S.; Fuhs, M.; Mobius, K. *J. Phys. Chem. A* **1997**, *101*, 5869–5876.
(91) Mazzoni, M.; Conti, F.; Corvaja, C. *Appl. Magn. Reson.* **2000**, *18*, 351–361.
(92) Ishii, K.; Ishizaki, T.; Kobayashi, N. *J. Chem. Soc., Dalton Trans.* **2001**, 3227–3231.
(93) Ishii, K.; Takeuchi, S.; Kobayashi, N. *J. Phys. Chem. A* **2001**, *105*, 6794–6799.
(94) Gouterman, M. Optical spectra and electronic structure of porphyrins and related rings. In *The Porphyrins*; Dolphin, D., Ed.; Academic Press: New York, 1978; Vol. *3*, pp 1−165.
(95) Kandrashkin, Y.; van der Est, A. *Chem. Phys. Lett.* **2003**, *379*, 574–580.
(96) Quimby, D. J.; Longo, F. R. *J. Am. Chem. Soc.* **1975**, *97*, 5111–5117.
(97) Asano, M.; Kaizu, Y.; Kobayashi, H. *J. Chem. Phys.* **1988**, *89*, 6567–6576.

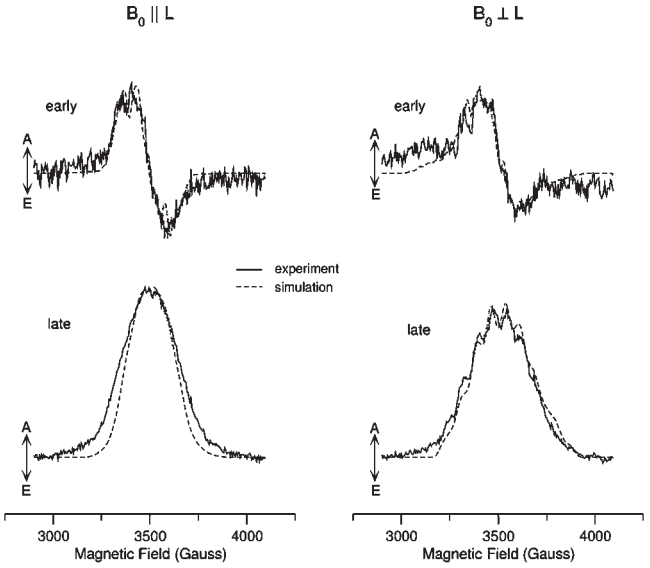

Figure 7. Spin-polarized transient EPR spectra of VOTTP-Vz. The spectra have been extracted from the experimental data sets by fitting the time traces with a function describing two sequential polarization patterns. The top traces are the polarization pattern that dominates at early times following the laser flash; the bottom traces are the pattern at late times. The spectra were measured at 20 K in the solid phase of the liquid-crystal 5CB and were frozen from the nematic phase in the presence of a magnetic field. In the left panel, the director of the liquid crystal is parallel to the magnetic field; in the right panel, the director and the field are perpendicular to each other. The dashed spectra are simulations. The early spectra (top) are calculated for the quintet state $^5Q_{T1}$ with D = 9.6 mT, $\kappa_{m,P}$ = 1.0, $\kappa_{m,\perp}$ = 0.0, and κ_n = 0.0. The late spectra are calculated for the triplet state $^3D_{S0}$ with the parameters given in the caption to Figure 3. The ordering due to the liquid crystal has been taken into account as described previously,[60] and the orientation distribution has been set to give the principal order parameter $S_{zz} = -0.28$.

These two possibilities can be distinguished by transient EPR measurements.

Figure 7 shows transient EPR spectra of VOTTP-Vz dissolved in the liquid-crystal 5CB and frozen from the nematic phase in the presence of a strong magnetic field. This results in a macroscopically aligned solid solution. The spectra on the left of Figure 7 are taken with the director of the liquid crystal parallel to the field ($L||B_0$), and for those on the right, the frozen sample has been rotated so that the ordering axis is perpendicular to the field ($L\perp B_0$). The observed polarization pattern changes with time, and the transients are described by the function

$$S(t, B_0) = \alpha(B_0)\, e^{-t/\tau_1} + \beta(B_0)\,(1 - e^{-t/\tau_1})e^{-t/\tau_2} \quad (9)$$

where τ_1 is the lifetime of the early signal and the rise of the late signal, τ_2 is the lifetime of the late signal, and $\alpha(B_0)$ and $\beta(B_0)$ are the spectra of the species observed at early and late times, respectively. A global fit of the time/field data set with τ_1 = 2.6 μs and τ_2 = 4 ms yields the experimental spectra shown in Figure 7. As can be seen, the early spectra (Figure 7, top) display primarily multiplet polarization while the late spectra (Figure 7, bottom) have purely absorptive net polarization. With the director perpendicular to the field, the normal to the plane of the porphyrin is expected to be aligned along the field and, hence, the largest component of the vanadium hyperfine coupling should be observed. A clear pattern of hyperfine peaks is visible in the late spectrum for this orientation (Figure 7, bottom right), and the observed splitting is consistent with that expected for the $^3D_{S0}$ state (i.e., the triplet state derived from the ground singdoublet state). This suggests that the transition from the early to late spectra is due to the decay of the quintet−triplet ($^5Q_{T1}/^3Q_{T1}$) manifold and that this process results in net polarization of the $^3D_{S0}$ state. Also shown in Figure 7 are simulations (dashed curves) of the experimental spectra (solid curves). The simulated spectra are calculated as described above for the triplet and tripquartet states. Good agreement is obtained by assuming that the early spectrum is the quintet state $^5Q_{T1}$ with predominantly multiplet polarization and values of D_{Qi} = 9.6 mT and E_{Qi} = 0 for the ZFS parameters. The late spectrum is simulated well as the $^3D_{S0}$ state with predominantly absorptive net polarization. The ZFS D_{Qi} of a quintet state formed from a triplet state coupled to two doublet states is given by[48]

$$D_{Qi} = \frac{1}{6}(D_T + D_{D_1T} + D_{D_2T}) + \frac{1}{12}D_{D_1D_2} \quad (10)$$

where D_T is the ZFS of the triplet state and D_{D_1T}, D_{D_2T}, and $D_{D_1D_2}$ are the dipolar couplings between the each of the doublets and the triplet and between the two doublet spins, respectively. Using eq 8, eq 10 can be rewritten in terms of the ZFS parameters of the quartet states formed by the coupling of the triplet to each of the two doublet states individually. For our case, this gives

$$D_{Qi} = \frac{1}{2}(D_{Qa}^{VOTTP} + D_{Qa}^{H_2TPP\text{-}Vz}) - \frac{1}{6}D_T^{H_2TPP} + \frac{1}{12}D_T^{VOTPP\text{-}Vz} \quad (11)$$

where D_{Qa} and D_T are the ZFS parameters for the respective quartet and triplet states. Using D_{Qa}^{VOTTP} = 17.5 mT,[60] $D_{Qa}^{H_2TTP\text{-}Vz}$ = 16.0 mT (Figure 5), $D_T^{H_2TTP}$ = 34.8 mT (Figure 5), and $D_T^{VOTTP\text{-}Vz} = -8.6$ mT (Figure 3) yields a value of D_{Qi} = 10.2 mT in good agreement with the value obtained from the simulation of the early spectra shown in Figure 7, confirming that it is indeed due to the quintet state.

The assignment of the early spectrum to the quintet state implies that it is the lowest excited state and therefore that all four electron spins become ferromagnetically coupled when the porphyrin is excited. Thus, the coupling between the metal and verdazyl radical is switched from antiferromagnetic to ferromagnetic by excitation of the porphyrin. However, the data suggest that the lifetime of the excited state is only about 2.6 μs at 20 K. The mechanism by which net polarization in the late signal is generated is uncertain. However, recently we reported the generation of net polarization in the excited tripquartet state of vanadyl octaethylporphyrin[59−61] and in the ground state of copper porphyrins.[67] In both cases, net polarization results from thermal equilibration between the tripquartet and tripdoublet states, and in the case of the copper porphyrins, it is then transferred to the ground state during decay of the excited states. In the case of VOTTP-Vz, thermal equilibration of the quintet, triplet, and singlet states derived from the tripdoublet and tripquartet states is also expected to generate net absorptive polarization, which can be transferred to the $^3D_{S0}$ state during electronic relaxation.

Transient EPR Spectra of CuTTP-Vz. For CuTTP-Vz, extremely broad, spin-polarized TREPR spectra displaying both multiplet and net polarization that evolve with time are obtained (see Figure S10 in the Supporting Information). For copper porphine, the ZFS in the lowest tripquartet state has been determined to be $|D| = 10-11$ GHz.[98] Thus, in CuTTP-Vz, the ZFS parameters of the quintet ($^5Q_{T1}$) and triplet states ($^3Q_{T1}$) derived from the porphyrin tripquartet state are expected to be similar in magnitude to the Zeeman interaction. This complicates the analysis of the spectra because the high-field approximation is no longer valid, and our description of the spin polarization cannot be applied. We are currently developing a model for spin polarization for these conditions and will report the analysis of the CuTTP-Vz spectra elsewhere.

Conclusions

The results presented here demonstrate that under favorable conditions light-induced spin-polarized EPR spectra of the excited states of a metal−radical complex can be observed and used to study the spin−spin interactions. This is an important development because there are few other methods that can distinguish the spin states when they are close in energy as in the current example. The behavior of the metalloporphyrin−verdazyl radical systems illustrates the challenges of assembling multispin complexes that can be photoswitched from one magnetic state to another. Because the verdazyl group orients nearly perpendicularly to the porphyrin ring, it experiences a weak antiferromagnetic spin−spin interaction with the metal in the porphyrin. On the one hand, this is advantageous because it allows this interaction to be switched transiently by the stronger ferromagnetic interaction with the porphyrin π electrons when the porphyrin is excited. On the other hand, the weak interaction means that even at low temperature rapid thermal equilibration between the spin states occurs, which promotes decay of the excited states. Other factors such as the spin−orbit coupling in the metal and the difference of the exchange interactions between the verdazyl radical and the two unpaired electrons mix the spin states and also tend to shorten the excited-state lifetime. The problem of rapid thermal equilibration can be improved if the coupling between the radical and photoexcitable moiety is made stronger. This may be possible by attaching the verdazyl radical so that it is coplanar with the porphyrin ring. Cooperative interactions within the solid are also essential, and the structure must be modified to allow the verdazyl radicals to come into closer contact.

Acknowledgment. We gratefully acknowledge support from NSERC (to A.v.d.E. and M.P.), the CRC (Tier II Canada Research Chair, to M.P.), CFI (to A.v.d.E. and M.P.), Brock University (International Grant, to M.P.), and the MEC (Ramon y Cajal research contract to A.A. and Juan de la Cierva research contract to V.P.).

Supporting Information Available: X-ray crystallographic data in CIF format, synthetic procedures, mass spectra, steady-state EPR spectra, UV/vis spectra, and cyclic voltammograms of the newly synthesized compounds, and transient EPR spectra of CuTTP-Vz. This material is available free of charge via the Internet at http://pubs.acs.org.

(98) van der Poel, W. A. J. A.; Nuijs, A. M.; van der Waals, J. H. *J. Phys. Chem.* **1986**, *90*, 1537–1540.
(99) Roos, B.; Sundbom, M. *J. Mol. Spectrosc.* **1970**, *36*, 8–25.